International Journal of Infrastructure Research and Management
Vol. 11 (1), June 2023 pp. 11 - 24

FINITE ELEMENT ANALYSIS OF REINFORCED CONCRETE BEAM-COLUMN CONNECTION WITH KINKED REBAR CONFIGURATION UNDER LATERAL CYCLIC LOADING USING ABAQUS

Norhaiza Nordin & Muhammad Zulhelmi Husaini Zahri Afandi
Infrastructure University Kuala Lumpur, MALAYSIA

ABSTRACT

Plastic hinge deformation is a mode of failure due to earthquake loading commonly found on beam-column joint of a reinforced concrete (RC) structure that adopted strong column-weak beam (SCWB) philosophy. This philosophy is widely used and have been the basic principles of many seismic codes. One research study conducted an experiment with a new steel reinforcement design with kinked configuration with the aim of relocating the plastic hinge deformation away from the beam-column joint to a desirable location on the beam. This design has the potential to improve the usable spaces of a building as stocky column design is no longer necessary. However, all experimental specimens by previous study were found to have only used a single type of concrete grade and the same cyclic loading. Therefore, the deformation of the newly proposed design is mostly unknown under various different conditions. This study aims to analyse the deformation of the new RC structure design under cyclic loading with the implementation of different parametric conditions through finite element modelling using ABAQUS. It was found that the deformation and cracking pattern of the simulated structures are in good agreement with the selected experimental specimen despite being under different conditions. Furthermore, the kinked rebar region was found to have a significant effect on the formation of the initial deformation of the structure under cyclic loading.

Keywords:
ABAQUS, Cracking pattern, Cyclic loading, Kinked rebar configuration, Strong column-weak beam

INTRODUCTION

The Strong Column Weak Beam (SCWB) is a design concept whereby the collapse of a building will not happen instantaneously but rather gradually, which will allow adequate time for the occupants to escape. The adaptation SCWB in most seismic codes have allowed plastic hinge deformation to occur on beam-column connection, preventing the formation of joint shear failure on the structural column (Arowojolu et al., 2019). However, deformation around structural columns during major seismic event is still possible. Therefore, a localised failure at the connecting beam away from the beam-column joint is a more preferred mode of failure than the formation of plastic hinge deformation (Rahman et al., 2016).

An experiment was conducted to analyse the deformation of Reinforced Concrete (RC) beam-column connection with kinked rebar configuration, a new design that is aimed to relocate the deformation away from the beam-column connection under cyclic loading (Qiang et al., 2019). However, even with promising results, the experiment was conducted with only several test samples using the same concrete grade and cyclic loading. Therefore, data on the effects of different conditions on the deformation of the structure are mostly unknown. As a result, further investigations on this new method are recommended due to its practicality and effectiveness in reducing the flexural capacity of the beam (Nie et al., 2020).

Thus, there is a need to analyse the behaviour of structural deformations of the newly proposed steel reinforcement configuration under various different conditions. Simulation modelling using finite element software such as ABAQUS would be more ideal and economical as experimental studies would prove to be costly and also impractical in the time of a pandemic outbreak.

ISSN Print: 2811-3608
ISSN Online: 2811-3705
https://iukl.edu.my/rmc/publications/ijirm/
DOI:10.63646/j.jdsti.2023110102

LITERATURE REVIEW

Damages sustained by RC structures after an earthquake event are mostly found in the region of beam-column connection (Feng et al., 2018 and Wong et al., 2008). They are mostly consistent with most simulation and experimental studies. These consistencies prove that structural cracking and deformation patterns are formed as a result of complex ground acceleration of seismic loading which can approximately be predicted even with simple cyclic loading patterns. Therefore, a new approach in structural design is required to avoid structural failures from occurring at the beam-column connection.

Qiang et al. (2019) proposed a novel kinked rebar configuration with the aim of relocating the plastic hinge deformation away from beam-column connection when an RC structure is damaged due to cyclic loading. The design introduces weak points on the structural beam which are strategically placed at the inflection point as the bending moment on the beam is due to vertical loading of zero. Double plastic hinge deformations were found on the beam where the rebars are kinked after the structure was subjected to cyclic loading. The experimental result obtained by Qiang et al. (2019) seemed to be promising as there was barely any deformation found on the beam-column connection.

Numerous research studies have been conducted to study the deformation behaviour of RC beam-column joint under cyclic loading. Luk & Kuang (2017) made three different types of finite element models of concrete beam-column structure using ABAQUS with all of them being subjected to cyclic loading. Feng et al. (2018) implemented finite element modelling using ABAQUS to analyse the cyclic behaviour of precast concrete beam-to-column connections using a newly proposed model. Wong & Kuang (2018) prepared seven RC beam-column T- shaped structures based on BS8110 for cyclic loading test with a 1000kN axial load acting on the column. Joyklad & Pimanmas (2011) prepared four RC beam-column joint specimens, all of which satisfy ACI 318. All specimens were subjected to cyclic loading by applying 500kN hydraulic actuator at the top of the column.

Papers covered by all of the researchers mentioned above have found that the mode of failure of RC beam-column connection under cyclic loading are heavily dependent on the structural design. Structures with small column sizes have a higher tendency to develop joint shear failure meanwhile structures with larger column sizes as a result of seismic code design will most likely form plastic hinge deformation at the beam-column connection. This study aims to analyse the deformation of the new RC structure design under cyclic loading with the implementation of different parametric conditions through finite element modelling using ABAQUS.

METHODOLOGY

The steps taken in this research methodology are commonly found in most study involving finite element modelling simulation (Senthuraman et al., 2017). Four models; M-1, M-2, M-3 and M-4 were modelled for the study. Dimensions of the reinforced concrete structure, steel reinforcing rebar spacing and configuration, load configuration and material properties of concrete and steel reinforcement were all modelled based on experimental specimen RCB-KB5 conducted by Qiang et al. (2019). However, it was assumed that the volume occupied by the foam used in the experimental study around the kinked rebar region to be hollowed to reduce the amount of difficulty and computational cost required for the simulation. Model M-1 was modelled closely to experimental specimen RCB-KB5 for verification purpose. Model M-2 was modelled with its kinked rebar region being constrained with concrete rather than having the region hollow. Model M-3 used concrete of higher grade than all other three simulated models. Model M-4 was subjected to a real-life earthquake ground acceleration instead of a simple laboratory cyclic loading that was applied to the other three simulated models. It was also subjected to 1000kN axial load at the top of the column and also a point

load of 7.5kN at the same location on the beam where cyclic loading for the other three models were being applied. The ground acceleration was applied at the base of the column and the direction of the movement was parallel to the beam. Figure 2 shows the dimension of the hollowed regions with a depth of 130mm as well as their corresponding positions in the structure.

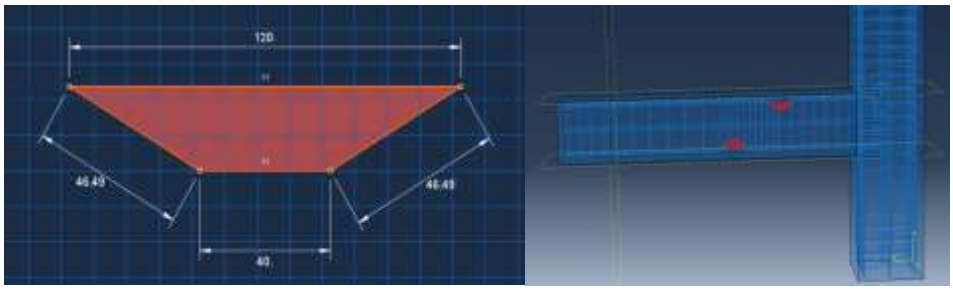

(a) (b)

Figure 2: (A) The Dimension of the Hollowed Region with A Depth of 130mm Used to Simulate the Foam Used in The Experimental Study (B) The Positions of Both Hollowed Region in The Structure as Replacement for The Foam Used in The Experimental Study

Concrete damaged plasticity (CDP) model was used to simulate the behaviour of concrete under cyclic loading. The compressive behaviour of the concrete as well as the damage parameters of both tension and compression required in ABAQUS were modelled based on the simplified damage plasticity model approach (Hafezolghorani et al., 2017). The tensile behaviour of the concrete was modelled using the bilinear tensile stress-crack width relationship (Walraven et al., 2013) Table 1 shows the values of plasticity parameters used in ABAQUS. Table 2 shows the data of tensile stress and its crack width relationship used in ABAQUS for all of the simulated models. Table 3 shows the data that are used to simulate the compressive behaviour of all four models.

Table 1: Values Of Plasticity Parameters Used In ABAQUS For CDP Approach

Dilation angle	Eccentricity	f_{b0} / f_{c0}	K	Viscosity Parameter
31	0.1	1.16	0.6667	0

Table 2: Data of tensile behaviour of concrete used in ABAQUS for all models

Concrete Tensile Behaviour Fracture Energy					
Model M-1, M-2 & M-4			Model M-3		
Tensile stress, σ_t (MPa)	Cracking width displacement, u_{ck} (mm)	Damage Parameter, d_t	Tensile stress, σ_t, (MPa)	Cracking width displacement, u_{ck} (mm)	Damage Parameter, d_t
0	0	0	0	0	0
3.765	0	0	4.561	0	0
0.7531	0.187	0.800	0.9123	0.161	0.800
0.038	0.933	0.990	0.046	0.803	0.990

Table 2: Compressive Stress, Inelastic Strain and Damage Parameter Data for All Models Used in ABAQUS

Concrete Compressive Behaviour					
Model M-1, M-2, M-4			Model M-3		
MPa			MPa		
Compressive stress, σ_c	Inelastic Strain, $\varepsilon_c^{in,h}$	Damage Parameter, d_c	Compressive stress, σ_c	Inelastic Strain, $\varepsilon_c^{in,h}$	Damage Parameter, d_c
19	0	0	24	0	0
21.000	0.0000765	0	28.000	0.0001232	0
23.000	0.0001577	0	30.000	0.0001895	0
25.000	0.0002444	0	32.000	0.0002595	0
27.000	0.0003382	0	34.000	0.0003341	0
29.000	0.0004409	0	36.000	0.0004142	0
31.000	0.0005558	0	38.000	0.0005013	0
33.000	0.0006887	0	40.000	0.0005977	0
35.000	0.0008523	0	42.000	0.0007071	0
37.000	0.0010898	0	44.000	0.0008369	0
38.000	0.0014142	0	48.000	0.0014142	0
36.000	0.0018730	0.0526	46.000	0.0018225	0.0417
34.000	0.0020631	0.1053	44.000	0.0019916	0.0833
32.000	0.0022089	0.1579	42.000	0.0021213	0.1250
30.000	0.0023319	0.2105	40.000	0.0022307	0.1667
28.000	0.0024402	0.2632	38.000	0.0023271	0.2083
26.000	0.0025381	0.3158	36.000	0.0024142	0.2500
24.000	0.0026282	0.3684	34.000	0.0024943	0.2917
22.000	0.0027120	0.4211	32.000	0.0025689	0.3333
20.000	0.0027907	0.4737	30.000	0.0026390	0.3750
18.000	0.0028652	0.5263	28.000	0.0027052	0.4167
16.000	0.0029360	0.5789	26.000	0.0027682	0.4583
14.000	0.0030037	0.6316	24.000	0.0028284	0.5000
12.000	0.0030686	0.6842	22.000	0.0028862	0.5417
10.000	0.0031310	0.7368			

All four models are subjected to cyclic loading. Model M-1, M-2 and M-3 are subjected to the same cyclic loading pattern. However, cyclic loading duration of Model M-1 and M-3 will only last up to 1.82 second which is considerably less than Model M-2 cyclic loading which is a full 18 second simulation due to the use of different meshing sizes and also to reduce extensive computational cost. Figure 4 shows the cyclic loading applied to Model M-1, M-2 and M-3. Figure 5 shows a section of Ranau Earthquake loading within the red boundary lines that was used on Model M-4 as a part of observing the structural deformation under real earthquake event.

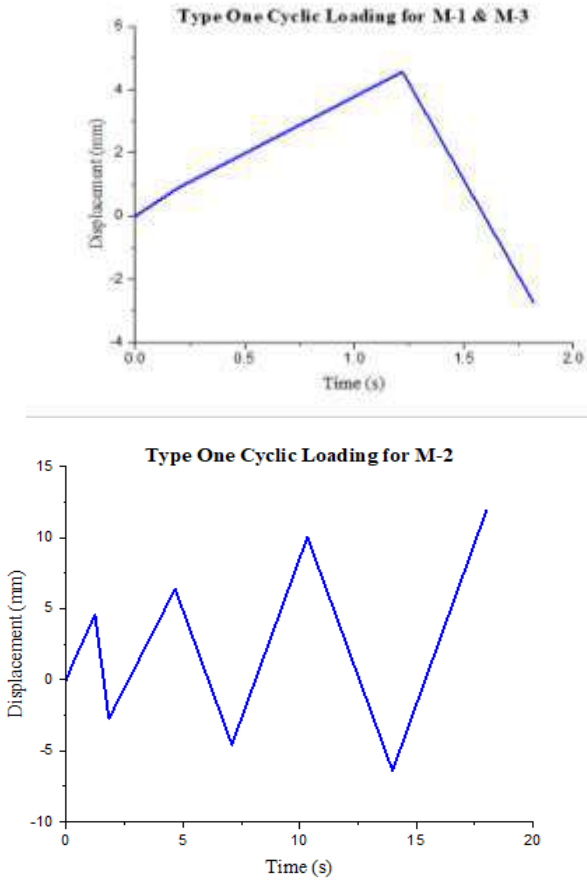

(a) (b)

Figure 4: (A) Cyclic Loading Applied to Model M-1 And Model M-3 (B) Cyclic Loading Applied to Model M-2

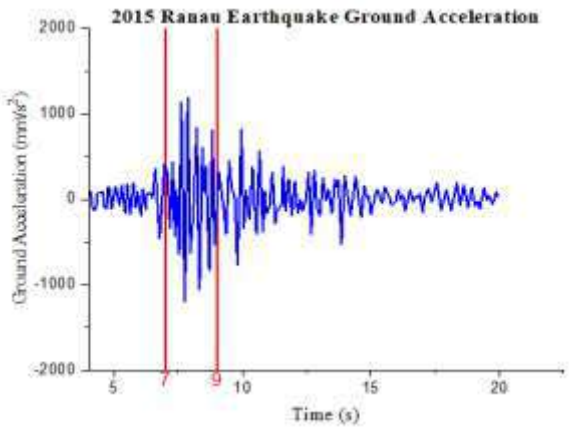

Figure 5: Selected Ranau Earthquake Ground Acceleration That Was Applied to Model M-4

ANALYSIS AND DISCUSSION

Deformation Patterns of All Finite Element Models

Cracking deformation patterns generated by ABAQUS for all four models are shown in Figure 6, 7, 8 and 9. Figure 10 and 11 show the structural deformation of specimen RCB-KB5 that were obtained experimentally for comparison purpose.

It was found that the cracking deformation of Model M-1 is in good agreement with the deformation found in the experimental study despite undergoing cyclic loading for only 1.82 second in the simulation. Model M-2 exhibits minor cracking deformation as compared to Model M-1 at 1.82 second into the simulation due to the additional concrete that constrains the kinked rebar region. However, a combination of severe cracking and crushing deformation can be seen on beam of Model M-2 after undergoing 18 second of cyclic loading. The location of most of the cracking are formed and can be seen in Figure 7(b) are mostly in good agreement with the experimental study despite Model M-2 having its kinked rebar region being fully constrained by concrete.

The cracking deformation pattern of Model M-3 is similar to that of Model M-1. However, cracking deformation is slightly more prominent in Model M-3 due to the use of higher concrete grade which tends to be more brittle (Kwan et al., 2004). Moreover, cracking deformation found on Model M-4 was only due to the 7.5kN point load exerted on the beam. No deformation was found on the column nor on any other parts of the structure due to earthquake ground acceleration. This could be due to the column's remarkable size despite being only 1.8m in height. Therefore, any column related damages due to buckling effect which are often found after an earthquake event could not be seen.

Cracking deformations obtained from all four simulated models heavily suggested that the kinked rebar configuration plays a significant effect on determining the location of the initial deformation of the structure. This is because bent-up steel reinforcement bars can reduce the structure's moment resistance. This finding is in good agreement with the results obtained by Galunic et al. (1977) and Yu & Tan (2014)

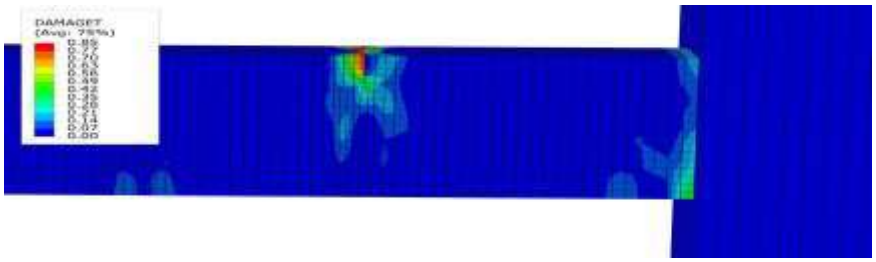

Figure 6: Cracking Deformation Pattern Produced by Model M-1 After Cyclic Loading Simulation (1.82 Second)

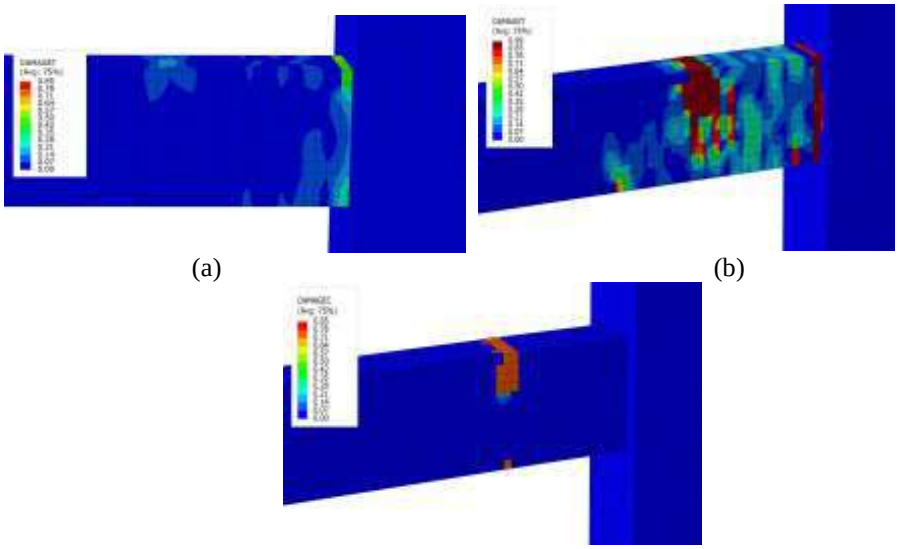

(a) (b)

(c)

Figure 7: (A) Cracking Deformation Pattern of Model M-2 At 1.82 Second Simulation (B) Cracking Deformation at 18 Second Simulation (C) Crushing Deformation Due to Compression

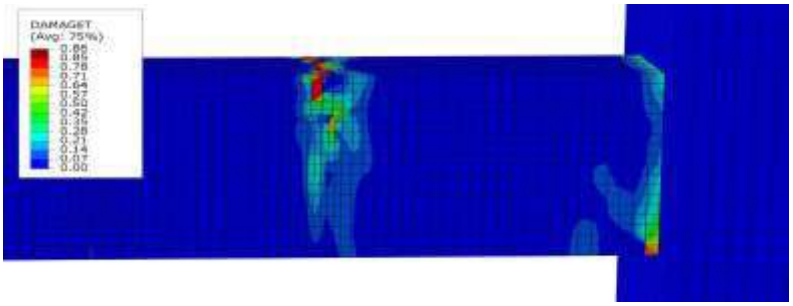

Figure 8: Cracking Deformation Pattern Produced by Model M-3 After Cyclic Loading Simulation (1.82 Second)

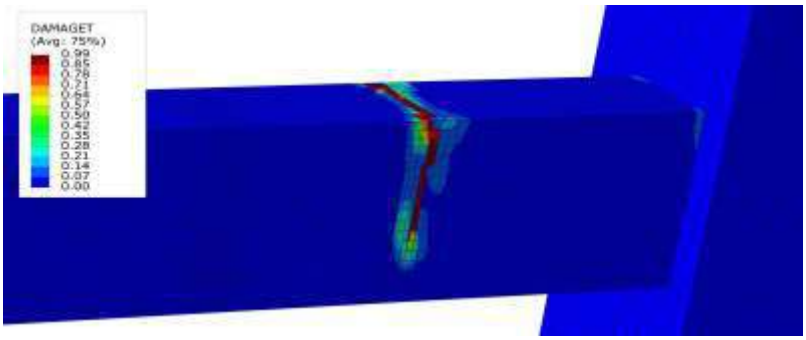

Figure 9: Cracking Deformation Pattern Produced by Model M-3 After Cyclic Loading Simulation (2.00 Second)

(a) (b)

Figure 10: Cracking Formation of Experimental Beam RCB-KB5 by Qiang et al. (2019) (A) Top View of the Beam (B) Bottom View of the Beam

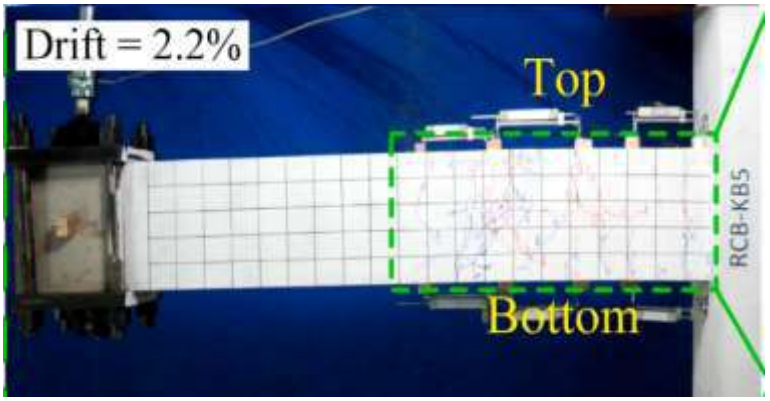

Figure 11: The Cracking Deformation Obtained from Experimental Study by Qiang et al. (2019)

Comparison of Load vs Displacement between Experimental & Analytical

Hysteresis loop of load vs displacement graph of model M-1 and model M-2 in comparison to the experimental result of specimen RCB-KB5 are shown in Figure 12 and Figure 13 respectively. It can be seen that the gradient of load vs displacement in both models are far steeper than the experimental load vs displacement. This is due the absence of pinching effect in the simulation, a phenomenon caused by shear deformation and steel reinforcement slippage along the adjacent of damaged concrete which is commonly found on structural members during reloading phased of a reversed cyclic loading (Deng et al., 2005). This finding is supported by Ab-Kadir et al. (2014) who found that hysteresis curve of load vs displacement obtained in ABAQUS/CAE could not simulate the pinching effect as properly as other finite element software.

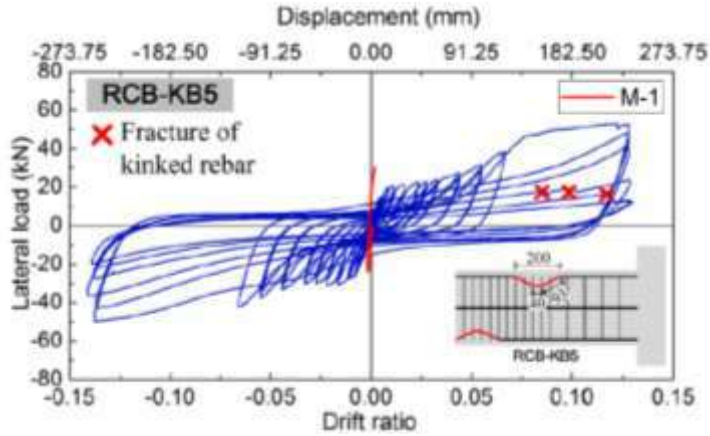

Figure 12: The Comparison of Load Vs Displacement of Model M-1 With Specimen RCB-KB5

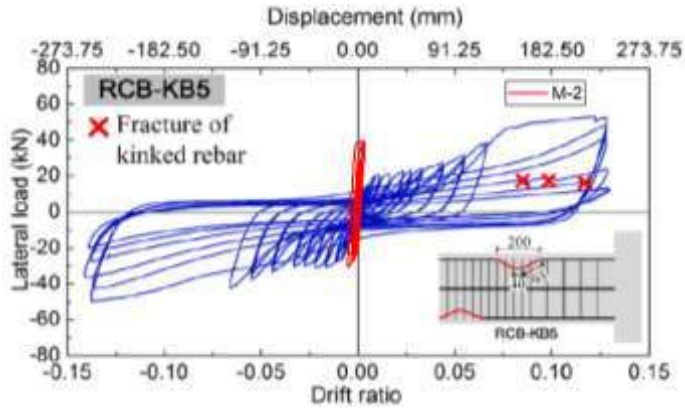

Figure 13: The Comparison of Load Vs Displacement of Model M-2 With Specimen RCB-KB5

Comparison of Load vs Displacement between Models

The comparison of hysteresis loop of load vs displacement between model M-1, M-2 and M-3 can be seen in Figure 14. The main graph shows the load vs displacement of all models with a simulation duration of 1.82 seconds. The smaller graph on the bottom right shows the load vs displacement of model M-1 and M-3 in conjunction with model M-2 18-second simulation. Model M-4 is kept separated as it was subjected under different cyclic loading and also analysed using different approach. All three models were subjected to a downward displacement of 4.559mm before the beam was subjected to the upward movement. The comparison of load vs displacement of model M-1 and model M-3 are mostly in good agreement as more forces are required to displace model M-3. This signifies that model M-3 has a higher stiffness than model M-1 as it uses higher concrete grade. However, specifically for the downward movement, model M-2 required the most amount of load for displacement compared to the other two models. This could be due to the reduction of flexural stiffness in model M-1 and M-3 due to the presence of hollowed regions. However, in the upward cyclic movement, model M-2 was found to be the least stiff out of the three. Although this result is against the author's initial prediction since the absence of hollowed regions should yield a higher

structural stiffness, it was found that the rate of load per unit displacement (stiffness) of all models were heavily dependent on the stress found in the steel reinforcement.

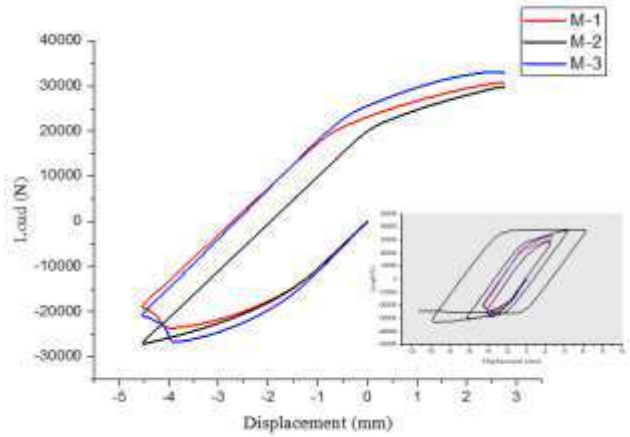

Figure 14: Load Vs Displacement of Model M-1, M-2 And M-3

Figure 15 shows the axial stress vs time of a selected steel reinforcement bar throughout the 1.82 second simulation. The negative stress magnitude indicates that the steel reinforcement is undergoing compression and vice versa. Maximum stress in steel reinforcement was found in model M-2 during the downward cyclic movement. However, it had the least amount of stress when the structure is moving in the upward direction which is completely consistent to the change in stiffness seen in Figure 14. The changes in structural stiffness and stress distribution in the steel reinforcement might be due to the straightening process of steel reinforcement undergone by model M-1 and M-3. This is because, plastic hinge moment capacity of the structure will gradually increase even after large deformation is found since the kinked reinforcement will try to straighten themselves as a result of cyclic movement (Peng et al., 2017). Steel reinforcement in model M-2 could not undergo the same straightening process due to the restraint of kinked reinforcement caused by the additional concrete.

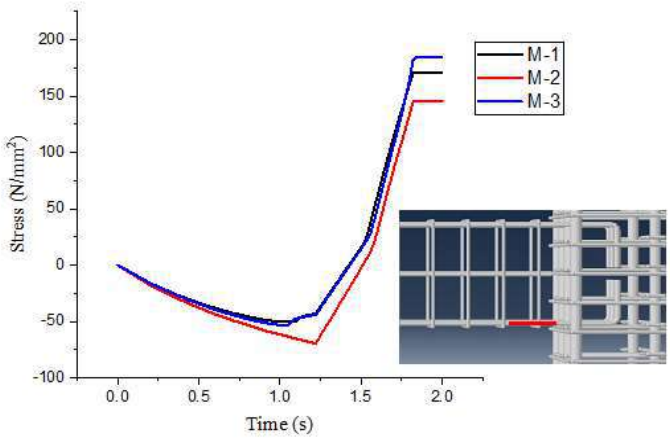

Figure 15: Stress Vs Time of the Selected Element of the Steel Reinforcement Shown in The Image

Figure 16 shows the vertical displacement of a selected node at the kinked reinforcement region throughout 1.82 second. The rate of vertical displacement is measured to compare the rate of straightening process undergone by the reinforcement steel of each model. The result shows a compelling evidence that stress in the steel reinforcement is heavily due to the straightening process. Therefore, the changes in stiffness in the structure is most likely due to the steel reinforcement straightening process. Although this theory is supported with compelling evidence, the sudden change in structural stiffness in a short cyclic period will most likely not happen. Thus, more researches are required to be conducted experimentally and analytically.

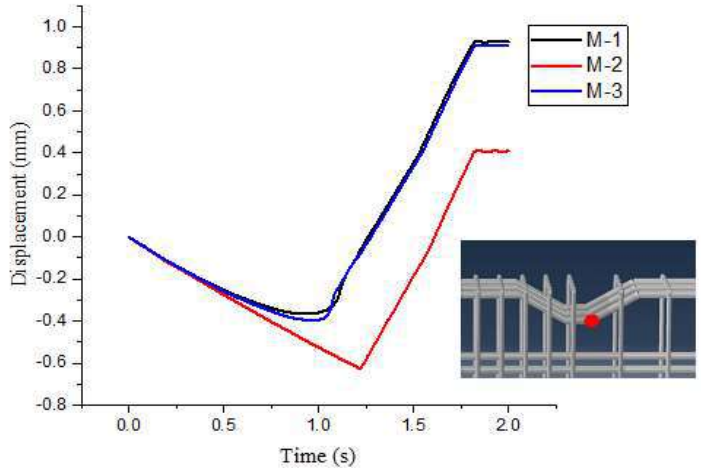

Figure 16: Vertical Displacement vs Time of the Selected Kinked Rebar Node Shown in The Image

Load vs Displacement of model M-4

Load vs displacement of model M-4 was analysed differently as the load could not be obtained through force reaction like the other three models. Therefore, nodal force due to stress element in the y-direction was chosen instead. Figure 17 shows the location of the nodal force. The red node was selected for the analysis as it was the closest to the point where cyclic movement was subjected on the other remaining models (blue node) as analysis could not be done on the exact same location.

Additional filtering is required to be conducted on model M-4 as the result consisted of high frequency noises. Mean values were taken for nodal forces that were recorded at the same time frame. It was found that the displacement of beam was mainly due to the 7.5kN point load and that the earthquake loading barely produce any movement in the y-direction due to vibration.

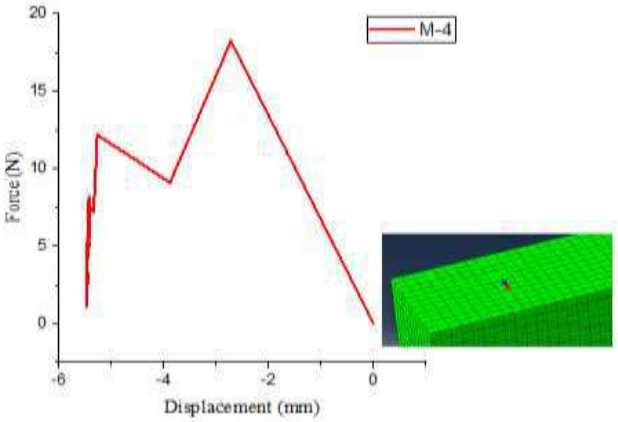

Figure 17: Load Vs Displacement of Model M-4

CONCLUSION AND RECOMMENDATION

The results of all simulation models have found that the kinked rebar configuration is capable of relocating the plastic hinge away from the beam-column joint to a more desirable location on the beam as described by Qiang et al. (2019) Simulation results have found compelling evidence that the kinked rebar configuration played a significant effect in triggering the initial deformation of the structure, despite being under different parametric conditions, due to its reduced moment capacity.

Cracking deformation on the simulated models are also in very good agreement with the experimental result. Most of the deformations are formed within the approximate region of the kinked steel reinforcement.

The comparison of load vs displacement of model M-1 and model M-2 in relative to specimen RCB-KB5 experimental result have shown differences particularly on the steepness of the gradient due to the absence of the pinching effect in ABAQUS CAE software application.

However, analytical comparison of load vs displacement between model M-1 and M-3 are as expected as model M-3 exhibited a stiffer structure due to the use of higher concrete grade. The structural stiffness of model M-2 fluctuated from being the stiffest out of the three (M-1, M-2 & M-2) in the initial downward cyclic movement to the least stiff as upward cyclic movement progresses. Results and data from ABAQUS indicated that it has a high level of correlation with the straightening process that potentially played a major impact in affecting the stress carried out by steel reinforcement in the structure.

No damages on model M-4 were associated to the seismic loading due to its remarkably large column size despite being only 1.8m in height. The damages seen on the beam are solely due to the point load.

It is recommended in the future that Manegotto-Pinto (M-P) model to be applied in ABAQUS to best simulate the slip-bond effect of concrete and steel reinforcement (pinching effect) (Filippou et al., 1983). Moreover, material properties in ABAQUS can be well defined through programming using UMAT sub-routine available in the software to improve the accuracy of the result (Feng et al., 2018).

AUTHOR BIOGRAPHY

Norhaiza Nordin, PhD is a lecturer in the Civil Engineering & Construction Department of Infrastructure University Kuala Lumpur. Dr. Norhaiza's research has focused on alleviating problems associated with reinforced design, construction and structural analysis. *Email: norhaiza@iukl.edu.my*

Muhammad Zulhelmi Husaini Zahri Afandi is a final year student at Infrastructure University Kuala Lumpur. He is studying in Bachelor of Civil Engineering (Hons)

REFERENCES

Ab-Kadir, M. A. Zhang, J. Mashros, N. Hassan, A. Mohd Yunus, N. & Aziz, N. (2014) "Experimental and Numerical Study on Softening and Pinching Effects of Reinforced Concrete Frame," *IOSR J. Eng.*, vol. 4, no. 5, pp. 01–05, doi: 10.9790/3021-04520105.

Arowojolu, O., Ibrahim, A., Rahman, M.K., Al-Osta, M. and Al-Gadhib, A.H (2019) "Plastic hinge relocation in reinforced concrete beam–column joint using carbon fiber–reinforced polymer," *Adv. Struct. Eng.*, vol. 22, no. 14, pp. 2951–2965, doi: 10.1177/1369433219855901.

Çelebi M., *et al.*, (2010) "Recorded motions of the 6 April Mw 6.3 L'Aquila, Italy, earthquake and implications for building structural damage: Overview," *Earthq. Spectra*, vol. 26, no. 3, pp. 651–684. doi: 10.1193/1.3450317.

Deng, H.Z. (2005) "A Simplified Method for Nonlinear Cyclic Analysis of Reinforced Concrete Structures: Direct and Energy Based Formulations," Heritage Branch, Ottawa, Canada.

Feng, D. C., Wu, G. & Lu, Y (2018) "Finite element modelling approach for precast reinforced concrete beam-to-column connections under cyclic loading," *Eng. Struct.*, vol. 174, no. May, pp. 49–66. doi: 10.1016/j.engstruct.2018.07.055.

Feng, P., Qiang, H., Qin, W.& Gao, M. (2017) "A novel kinked rebar configuration for simultaneously improving the seismic performance and progressive collapse resistance of RC frame structures," *Eng. Struct.*, vol. 147, pp. 752–767, doi: 10.1016/j.engstruct.2017.06.042.

Filippou, F. C., Popov, E. P. & Bertero, V. V. (1983) "Effects of bond deterioration on hysteretic behavior of reinforced concrete joint (EERC 83-19)," University of California, Berkeley,

Galunic, B., Bertero, V. V. & Popov, E. P. (1977) "An Approach for Improving Seismic Behavior of Reinforced Concrete Interior Joints," University of California, Berkeley

Hafezolghorani, M., Hejazi, F. Vaghei, R., Jaafar, M. S. and Karimzade, K. (2017) "Simplified damage plasticity model for concrete," *Struct. Eng. Int.*, vol. 27, no. 1, pp. 68–78. doi: 10.2749/101686616X1081.

Joyklad, P. & Pimanmas, A. (2009) "Cyclic stress development in substandard beam-column joint," *Proc. Inst. Civ. Eng. Struct. Build.*, vol. 164, no. 3, pp. 211–225, 2011, doi: 10.1680/stbu.9.00055.

Kwan, A. K. H., Ho, J. C. M. & Pam, H. J. (2004) "Effects of concrete grade and steel yield strength on flexural ductility of reinforced concrete beams," *Aust. J. Struct. Eng.*, vol. 5, no. 2, pp. 1–20. doi: 10.1080/13287982.2004.11464932.

Luk, S.H. & Kuang, J. S. (2017) "Seismic performance and force transfer of wide beam-column joints in concrete buildings," *Proc. Inst. Civ. Eng. Eng. Comput. Mech.*, vol. 170, no. 2, pp. 71–88, doi: 10.1680/jencm.15.00024.

Majid, T. A., Adnan, A. Adiyanto, M. I., Ramli, M. Z. and Ghuan, T. C. (2015) "Preliminary Damage Assessment Due to Ranau Earthquake," *Int. J. Civ. Eng. Geotech.*, vol. NCWE2017, no. 9, pp. 1–6, 2017, [Online]. Available: http://ijceg.ump.edu.my.

Nie, X., Zhang, S., Jiang, T., and Yu, T. (2020) "The strong column–weak beam design philosophy in reinforced concrete frame structures: A literature review," *Adv. Struct. Eng.*, vol. 23, no. 16, pp. 3566–3591. doi: 10.1177/1369433220933463.

Qiang, H., Feng, P., Stojadinovic, B., Lin, H., and Ye L., (2019) "Cyclic loading behaviors of novel RC beams with kinked rebar configuration," *Eng. Struct.*, vol. 200, Dec. doi: 10.1016/j.engstruct.2019.109689.

Rahman, M.K., Arowojolu, O.S., Baluch, M.H., Gadhib, A.H., and Al-Osta, M. (2016) "Relocating the plastic hinge abeam column joint interface into the beam in CFRP strengthening," *Proc. 8th Int. Conf. Fibre-Reinforced Polym. Compos. Civ. Eng. CICE*, no. December, pp. 1024–1032.

Sethuraman, V.S, Suguna, K, and Raghunath P.N., (2017) "Numerical Analysis of High strength concrete with Cyclic loading using Abaqus," *Glob. J. Pure Appl. Math.*, vol. 13, no. 2, pp. 225–235. [Online]. Available: http://www.ripublication.com.

Walraven, J. & Bigaj-van Vliet, A (2010) *Model Code for Concrete Structures* Berlin, Germany: Wilhelm Ernst & Sohn Verlag für Architektur und technische Wissenschaften GmbH & Co. KG,

Wong, H. F. & Kuang, J. S. (2008) "Effects of beam-column depth ratio on joint seismic behaviour," *Proc. Inst. Civ. Eng. Struct. Build.*, vol. 161, no. 2, pp. 91–101, doi: 10.1680/stbu.2008.161.2.91.

Yu, J. & Tan, K. H. (2014) "Special Detailing Techniques to Improve Structural Resistance against Progressive Collapse," *J. Struct. Eng.*, vol. 140, no. 3, p. 04013077. doi: 10.1061/(ASCE)st.1943-541x.0000886.